engineering proceedings

MDPI

Proceeding Paper

Alternating Sequential Model Predictive Control in Multimodular Direct Matrix Converters †

Rodrigo Romero [1,*], Edgar Maqueda [1], Sergio Toledo [1], Carlos Romero [1], Sergio Núñez [1], Raúl Gregor [1] and Marco Rivera [2]

[1] CITHED, Department of Electronic and Mechatronic Engineering, Facultad de Ingeniería, Universidad Nacional de Asunción, San Lorenzo 2160, Paraguay; emaqueda@ing.una.py (E.M.); stoledo@ing.una.py (S.T.); cromero@ing.una.py (C.R.); snunez@ing.una.py (S.N.); rgregor@ing.una.py (R.G.)
[2] Power Electronics, Machines and Control (PEMC) Research Institute, Nottingham NG7 2QL, UK; marco.rivera@nottingham.ac.uk
* Correspondence: rnromero@fiuna.edu.py
† Presented at the 6th International Electronic Conference on Applied Sciences, 9–11 December 2025; Available online: https://sciforum.net/event/ASEC2025.

Abstract

This work presents an alternating sequential model predictive control (ASMPC) scheme applied to multimodular matrix converters. The proposed strategy alternately evaluates two control objectives: load current tracking and input reactive power minimization. The algorithm was implemented in MATLAB/Simulink on an architecture composed of two direct matrix converters in a multimodular configuration. The influence of parameter N_2 on system performance was analyzed under step changes in reference current of 30 A and 60 A. To this end, performance metrics such as THD and MSE were used, along with a descriptive statistical analysis including the mean, standard deviation, mean absolute deviation (MAD), and coefficient of variation (CV). Simulation results show stable performance for variations in N_2, with an input current THD of 8.10% and load THD reduced to 1.00%, demonstrating improved harmonic performance compared with classical weighted MPC approaches.

Keywords: model predictive control; matrix converter; alternating sequential control; reactive power; multimodular converters

1. Introduction

Direct matrix converters (DMCs) enable direct AC–AC power conversion without a DC-link stage, allowing high power density, bidirectional power flow, and controllable input power factor [1]. Due to these characteristics, they have been widely considered for applications in motor drives, renewable energy interfaces, and aerospace systems [2–5]. However, in medium- and high-power scenarios, single-converter implementations present limitations related to scalability, thermal stress distribution, and fault tolerance. To address these limitations, multimodular direct matrix converter (MMDMC) architectures have received increasing attention, where two or more DMCs operate in parallel [6,7]. This approach improves rated power capability, reliability, and fault-tolerant operation by redistributing the load among healthy modules [8]. Nevertheless, it increases control complexity, since the control strategy must simultaneously guarantee output current tracking, input reactive power mitigation, and stable operation under multiple admissible switching states. Recent research on control strategies for matrix converters can be classified into four

Academic Editor: Alessandro Lo Schiavo

Published: 30 March 2026

main approaches. The first corresponds to weighted finite-control-set model predictive control (FCS-MPC), which is widely adopted due to its capability to handle system constraints and nonlinear converter behavior in real time [9,10]. However, its main limitation lies in the sensitivity to the tuning of weighting factors, which is typically performed empirically and depends on the operating point. A second group includes intelligent or optimization-assisted techniques. Neural networks assist weighting-factor selection [11], fuzzy logic adapts weights online [12], and genetic algorithms improve switching-state selection [13]. These approaches can improve multi-objective performance but increase computational burden and implementation complexity. A third approach corresponds to sequential or hierarchical model predictive control (SMPC), which reduces the need for explicit weighting-factor tuning by prioritizing control objectives [14]. Despite this advantage, its performance depends on the predefined priority order, which may become suboptimal when operating conditions change. Finally, alternating-sequence predictive control approaches evaluate control objectives alternately between consecutive sampling instants [15], thereby mitigating the bias associated with fixed priorities. Nevertheless, the robustness of these strategies in multimodular architectures and under variations in switching-state sets has not yet been sufficiently quantified. The literature still lacks a structured comparative analysis of weighted, intelligent tuning, sequential, and alternating control strategies, as well as a statistical robustness assessment for MMDMCs. This study proposes an alternating sequential model predictive control (ASMPC) approach for output current tracking and input reactive power minimization. Performance is evaluated using THD, MSE, and descriptive statistics across valid switching-state sets.

2. Methods

2.1. System Description and Predictive Control Model

The topology shown in Figure 1 contains two three-phase MC modules connected to the six-phase wind generator (SpWEG), which has two sets of three-phase windings with isolated neutral points. Therefore, in the proposed topology, three phases of the SpWEG are connected to one module and the other three phases are connected to the other module, each with its respective neutral. The SpWEG is first connected to a passive Input Filter (RLC) with a damping resistor R_d to attenuate the resonance effects on the Input Filter (IF) of the matrix converter; after the matrix converter, an inductive Output Filter (OF) is connected. The filter outputs are then interconnected at the common connection point, where the current provided by both modules is added to power the load. The voltages generated by the SpWEG are denoted by the parameters u_1, v_1, and $w_1 \in v_{s1}$ for the 3 phases corresponding to the circuit of Module 1, and the parameters u_2, v_2, w_2, and $\in v_{s2}$ for the other 3 phases corresponding to the Module 2 circuit. The voltages v_{sx} where $x \in \{1,2\}$, and the currents i_{sx} where $x \in \{1,2\}$, are the measurements taken at the inlet of the IF, whose parameters are of interest for the determination of the reactive power.

The voltages v_{ix} where $x \in \{1,2\}$, and the currents i_{ix} where $x \in \{1,2\}$, are the measurements taken at the outlet of the IF, whose parameters are of interest for the determination of the reactive power. These parameters are taken into account to be entered into the predictive control model and instantaneous reactive power at the input is obtained.

The MC's input voltages are v_{ixu},v_{ixv}, and v_{ixw}, and the input currents are i_{ixu},i_{ixv}, and i_{ixw}, respectively. The output voltages of the MC with respect to the corresponding SpWEG neutral point (n_1 or n_2) are v_{oxa},v_{oxb} and v_{oxc}. In addition, the output currents are i_{oxa},i_{oxb}, and i_{oxc}, respectively. Finally, the OF voltages, or those on the load side, are v_{ga},v_{gb}, and v_{gc}.

https://doi.org/10.3390/engproc2026124093

Each MC consists of nine bidirectional switches. To avoid short circuits between the input lines, there are only 27 feasible switching states [16]. We define three-phase voltage and current vectors as follows:

$$\mathbf{v}_{ix} = \begin{bmatrix} v_{ixu} \\ v_{ixv} \\ v_{ixw} \end{bmatrix}, \mathbf{v}_{ox} = \begin{bmatrix} v_{oxa} \\ v_{oxb} \\ v_{oxc} \end{bmatrix}, \mathbf{v}_g = \begin{bmatrix} v_{ga} \\ v_{gb} \\ v_{gc} \end{bmatrix} \mathbf{i}_{ix} = \begin{bmatrix} i_{ixu} \\ i_{ixv} \\ i_{ixw} \end{bmatrix}, \mathbf{i}_{ox} = \begin{bmatrix} i_{oxa} \\ i_{oxb} \\ i_{oxc} \end{bmatrix}, \tag{1}$$

The relationship between the input and output voltages and currents of the matrix converter is determined by its switching state matrix $\mathbf{S}$. Specifically, the output voltage vector and the input current vector are given by $\mathbf{v}_{ox} = \mathbf{S} \cdot \mathbf{v}_{ix}$ and $\mathbf{i}_{ix} = \mathbf{S}^T \cdot \mathbf{i}_{ox}$. The switching functions and operational constraints of the $\mathbf{S}$ array, including the prevention of short circuits at the input, are fully defined in [8].

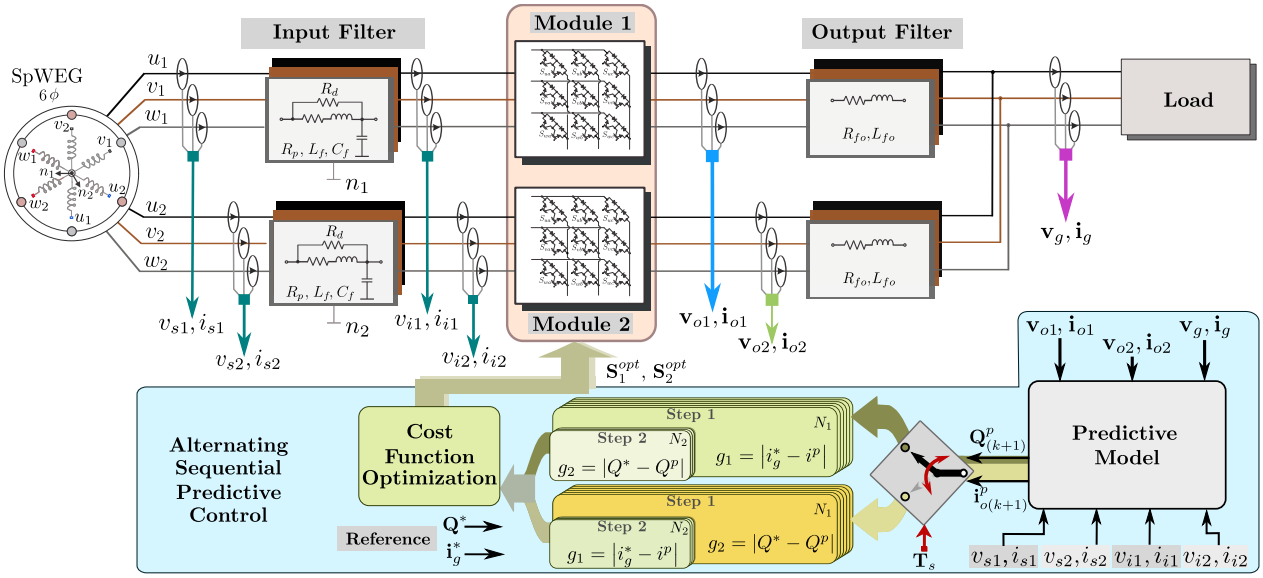

Figure 1. Topology of the proposed control scheme. Arrow colors are consistent with the measured variables shown in the results. The red arrow indicates the sampling period T_s.

2.2. Discrete Predictive Model of the MMDMC

The predictive model is derived from the continuous-time equations of the IF, the switching matrix, and the OF of the three-phase direct matrix converter. Since these formulations are well established, only the discrete-time expressions required for predictive control are presented [17]. The OF current for each module is predicted using forward Euler discretization:

$$\mathbf{i}_{ox}(k+1) = \left(1 - \frac{R_{fo}T_s}{L_{fo}}\right)\mathbf{i}_{ox}(k) + \frac{T_s}{L_{fo}}\left(\mathbf{v}_{ox}(k) - \mathbf{v}_g(k)\right) \tag{2}$$

T_s is the sampling time, $i_{ox}(k)$ and $v_g(k)$ are measured, and $v_{ox}(k)$ is calculated for all switching combinations in order to predict the next value of the output current and evaluate the cost function to select the optimal solution. Since reactive power minimization is a control objective, the IF predictive model is included. Estimating input reactive power (Q) at the next sampling instant requires prediction of both IF current and voltage. The corresponding discrete-time IF prediction equations are:

$$\begin{aligned} v_{ix}(k+1) &= a_{11}v_{ix}(k) + a_{12}i_{sx}(k) + b_{11}v_{sx}(k) + b_{12}i_{ix}(k) \\ i_{sx}(k+1) &= a_{21}v_{ix}(k) + a_{22}i_{sx}(k) + b_{21}v_{sx}(k) + b_{22}i_{ix}(k) \end{aligned} \tag{3}$$

$v_{sx}(k)$ is the measured supply voltage, and $i_{ix}(k)$ is calculated for each switching combination from the switching matrix **S**. The parameters a_{ij} and b_{ij} are obtained from the discretization of the filter's continuous-time model, as detailed in [17].

2.3. ASMPC Strategy and Algorithm Description

Conventional FCS-MPC strategies address multi-objective control using weighted cost functions, whose tuning is typically empirical and operating-point-dependent. Sequential MPC (SMPC) avoids explicit weights through hierarchical evaluation, although fixed objective priorities may introduce bias under varying operating conditions. To overcome these limitations, the proposed alternating sequential model predictive control (ASMPC) alternates the priority of the control objectives at consecutive sampling instants, enabling balanced multi-objective regulation without weighting factors. In addition, a candidate-state reduction stage (N_2) is introduced to decrease the computational burden while preserving the most relevant switching states, improving real-time feasibility for multimodular matrix converter systems.

Let $k \in \mathbb{N}_0$ be the sampling index, with $t_k = kT_s$ and T_s the sampling period. At each t_k, ASMPC evaluates admissible switching states under two objectives: output current tracking and input reactive power minimization. Rather than a weighted multi-objective cost, both criteria are applied sequentially, and their evaluation order alternates with the parity of k. The controller uses both predictive models. The Input Filter (IF) model predicts i_{sx} and v_{ex} to estimate and reduce future reactive power, while the Output Filter (OF) model predicts output current to preserve tracking accuracy at the load side.

At each sampling instant k, the following sequence is executed:

1. **Determination of the evaluation order**
   The priority order of the control objectives is determined according to the sampling index parity

$$\begin{cases} k \text{ odd:} & \text{first evaluate } g_1 \text{ then } g_2 \\ k \text{ even:} & \text{first evaluate } g_2 \text{ then } g_1 \end{cases}$$

   This alternating mechanism prevents a permanent priority bias between the control objectives.
2. **Evaluation of the first control objective**
   One of the main objectives is the regulation of the output current of each matrix converter module. Since the desired current delivered to the load is the sum of the currents of both modules, the reference current for each module is defined as:

$$\mathbf{i}_{ox}^{*} = \frac{\mathbf{i}_{g}^{*}}{2} \tag{4}$$

   $\mathbf{i}_{ox}^{*}$ denotes the reference current of module x ($x \in \{1,2\}$); and $\mathbf{i}_{g}^{*}$ corresponds to the load or grid current reference [8]. For control implementation, the measured three-phase variables are transformed into the $(\alpha - \beta)$ stationary reference frame [17]. Considering the $N_1 = 27$ admissible switching states of the matrix converter, the cost function associated with the output current control is evaluated for each state:

$$g_1 = (i_{ox\alpha}^{*} - i_{ox\alpha})^2 + \left(i_{ox\beta}^{*} - i_{ox\beta}\right)^2 \tag{5}$$

   where $i_{ox\alpha}^{*}$ and $i_{ox\beta}^{*}$ are the reference currents in the $\alpha - \beta$ plane, while $i_{ox\alpha}$ and $i_{ox\beta}$ correspond to the predicted output currents of module x, with $x \in \{1,2\}$ representing MC1 and MC2, respectively.

https://doi.org/10.3390/engproc2026124093

After evaluating all switching states, a reduced subset containing the N_2 states with the lowest values of g_1 is selected. This preselection stage significantly reduces the computational burden of the second evaluation stage while retaining the most promising candidate states.

3. **Evaluation of the second control objective**
For the N_2 preselected switching states, the second control objective related to reactive power minimization is evaluated. The corresponding cost function is defined as:

$$g_2 = \left| Q^* - Q^P(k+1) \right| \tag{6}$$

where Q^* is the reactive power reference and $Q^P(k+1)$ is the predicted reactive power at the next sampling instant. In this work, the reference value is defined as $Q^* = 0$ to enforce unity power factor operation. The reactive power is predicted as:

$$Q(k+1) = v_{s\alpha}(k+1) i_{s\beta}(k+1) - v_{s\beta}(k+1) i_{s\alpha}(k+1) \tag{7}$$

Here, $v_s(k+1)$ and $i_s(k+1)$ correspond to the predicted source voltage and current components in the $\alpha - \beta$ reference frame. Thus, the cost function is written as:

$$g_2 = \left(v_{sx\alpha} i_{sx\beta} - v_{sx\beta} i_{sx\alpha} \right)^2 \tag{8}$$

4. **Optimal switching state selection**
The optimal switching state is selected as the one that minimizes the second cost function g_2 among the N_2 candidate states. The corresponding switching configuration is then applied to the converter.
5. **Alternating repetition**
At the next sampling instant $k+1$, the evaluation order between g_1 and g_2 is reversed. By alternating the priority between consecutive sampling instants, the proposed ASMPC strategy distributes the control effort between both objectives over time, reducing the bias associated with fixed-priority sequential MPC approaches.

3. Results and Discussion

The performance of the proposed ASMPC strategy applied to the MMDMC system is evaluated by simulations performed in MATLAB/Simulink R2023b over 0.4 s, using the electrical parameters specified in Table I of [17], and the sampling frequency is set to 40 kHz to enable direct comparison with the results reported in the cited work. The analysis addresses the main operating conditions and the sensitivity to N_2.

3.1. Dynamic Performance

Figure 2a presents the average THD values of the input and output currents as a function of the parameter N_2. The results indicate that the output current THD remains practically unchanged across the evaluated range, showing that the proposed strategy preserves harmonic performance even when the number of candidate states is reduced.

Figure 2b shows the predicted load current ($i_g = 20$ A) and the currents supplied by each module ($i_{L_{1,2}} = 10$ A), compared with their respective references. The results confirm correct current sharing between modules, with each module contributing half of the total load current.

To assess the dynamic response, a step change in the current reference is introduced at $t = 0.2$ s, increasing the reference from $\mathbf{i}_g^* = 20$ A to $\mathbf{i}_g^* = 40$ A. The controller rapidly tracks the new reference while maintaining stable operation and balanced current distribution.

https://doi.org/10.3390/engproc2026124093

Reactive power minimization is activated at $t = 0.1\,\text{s}$. As shown in Figure 2c,d, the reactive power is effectively reduced after this instant while the current tracking performance remains stable. These results demonstrate that the alternating evaluation of the control objectives allows simultaneous regulation of current and reactive power without requiring weighting factors.

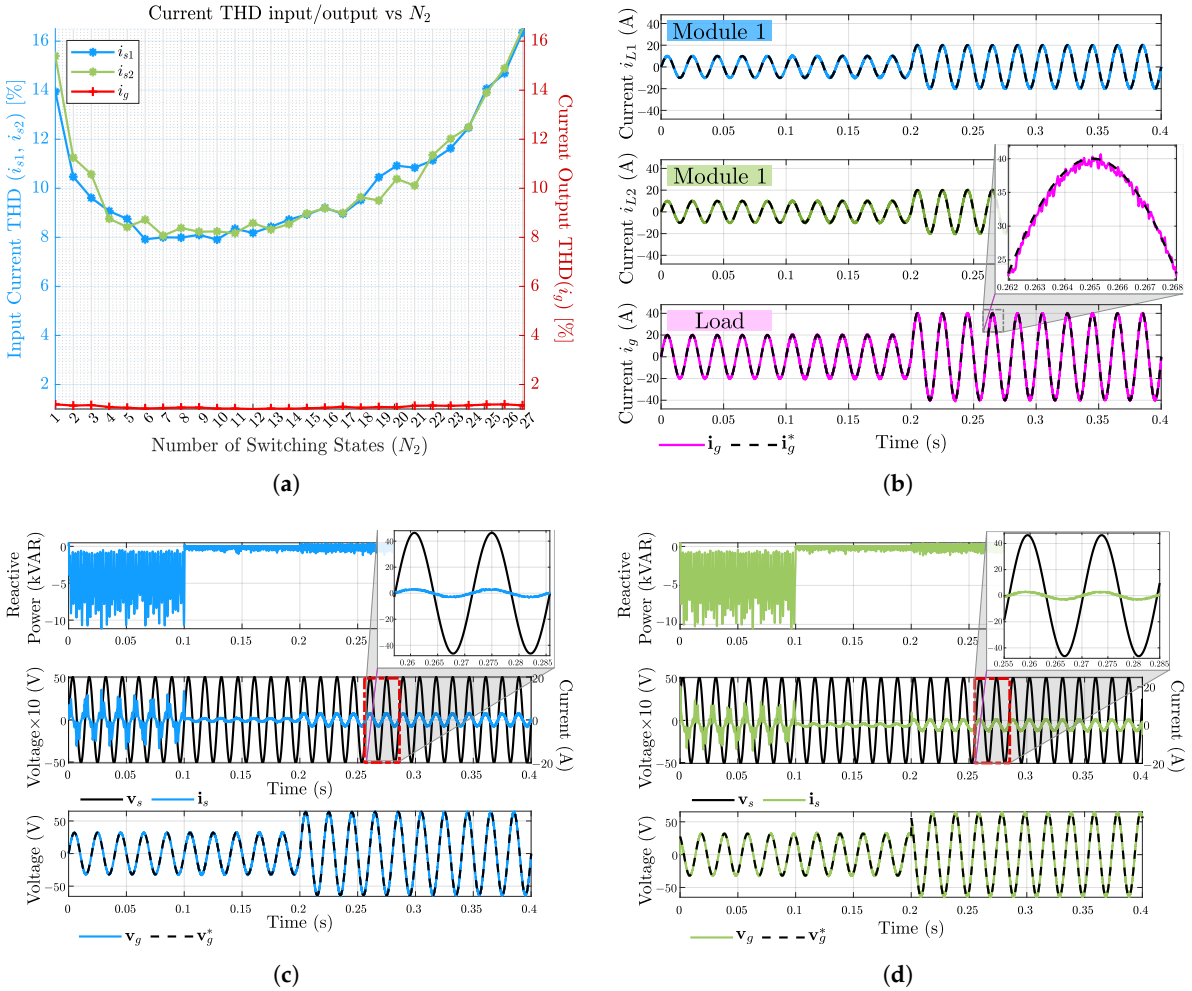

Figure 2. Dynamic performance of the proposed control strategy: (**a**) THD source and grid currents; (**b**) output current of each module and current at the load; (**c**) input reactive power, generator-side voltage and current, and output voltage for module 1; (**d**) input reactive power, generator-side voltage and current, and output voltage for module 2. Red dashed rectangles indicate zoomed-in regions, highlighting waveform behavior under increased current conditions.

3.2. Sensitivity Analysis with Respect to N_2

The parameter N_2 determines the number of candidate switching states considered during the second stage of the optimization process. To evaluate its influence, 27 simulations were performed by varying N_2 under two current reference levels: $\mathbf{Iref}_1 = 30\,\text{A}$ and $\mathbf{Iref}_2 = 60\,\text{A}$. Two figures of merit (FMs) were analyzed: the total harmonic distortion (THD) and the mean squared error (MSE) between the reference and predicted currents [18,19]. Since deterministic simulations are considered, descriptive statistics were used to evaluate system sensitivity, including the mean (μ), standard deviation (σ), variance (σ^2), mean absolute deviation (MAD), and coefficient of variation (CV), summarized in Table 1.

The obtained results show low dispersion of both THD and MSE across the evaluated conditions. The CV values remain between 4.97% and 13.56%, indicating consistent system

performance for different N_2 values. Furthermore, slightly lower dispersion is observed for the higher reference current (60 A), suggesting increased robustness under more demanding operating conditions. These results are supported by the statistical interpretation of dispersion indicators. According to [20], a CV between 8% and 14% is considered acceptable, while lower values indicate reduced variability. Similarly, [21] associates lower dispersion with greater consistency. In this context, the obtained CV values confirm statistically stable system behavior. This is further illustrated in Figure 3a, which shows the output THD with respect to the normative limit, and Figure 3b, which presents the MSE variability, where narrower bands indicate more consistent performance.

Table 1. Descriptive statistical parameters for the figures of merit: THD and MSE per phase.

	THD [%]						**MSE**					
	Iref$_1$			**Iref$_2$**			**Iref$_1$**			**Iref$_2$**		
Metric	I_a	I_b	I_c	I_a	I_b	I_c	I_a	I_b	I_c	I_a	I_b	I_c
Maximum	2.460	2.420	2.510	1.190	1.210	1.180	0.418	0.404	0.409	2.095	2.080	2.058
Minimum	1.930	1.940	1.940	0.980	1.000	1.000	0.286	0.276	0.276	1.673	1.696	1.688
Range	0.530	0.480	0.570	0.210	0.210	0.180	0.133	0.128	0.133	0.422	0.385	0.371
μ	2.199	2.192	2.188	1.083	1.089	1.086	0.347	0.344	0.343	1.802	1.800	1.799
σ	0.164	0.148	0.161	0.061	0.066	0.059	0.047	0.046	0.046	0.089	0.084	0.083
σ^2	0.027	0.022	0.026	0.004	0.004	0.003	0.002	0.002	0.002	0.008	0.007	0.007
MAD	0.147	0.130	0.136	0.052	0.056	0.051	0.043	0.042	0.042	0.062	0.055	0.054
CV [%]	7.449	6.737	7.338	5.603	6.040	5.416	13.564	13.357	13.430	4.966	4.639	4.636

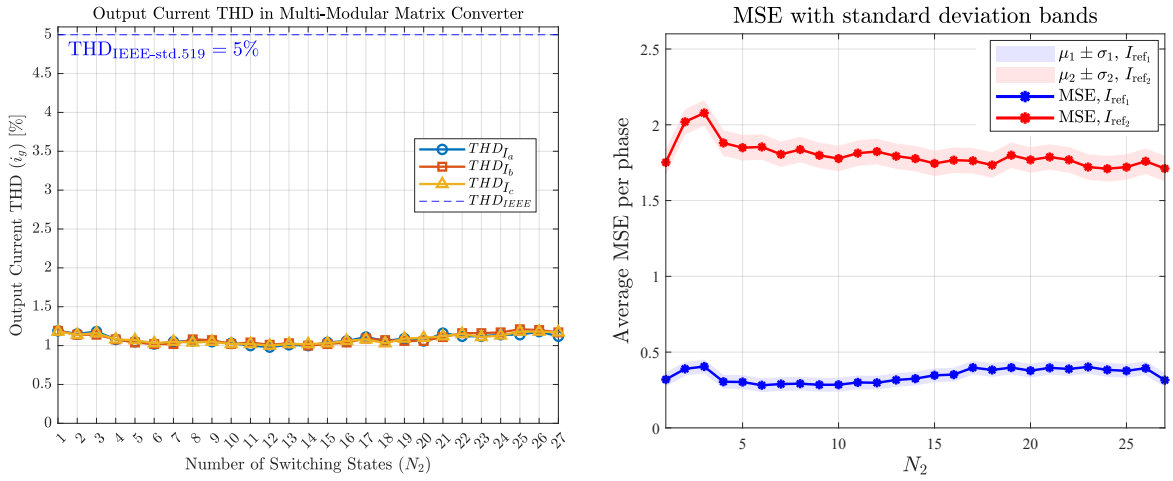

(**a**) (**b**)

Figure 3. Performance indices of the proposed control strategy: (**a**) current THD; (**b**) average mean squared error per phase.

3.3. Discussion

Compared with conventional weighted FCS-MPC strategies, the proposed ASMPC approach eliminates the need for empirically tuned weighting factors by alternating the evaluation of control objectives, which reduces priority bias and improves the balance between current tracking and reactive power minimization. The obtained results confirm the effectiveness of the proposed method. The input current THD in both modules is 8.10%, while the load THD is reduced to 1.00%. In comparison, the classical MPC strategy reported in [17] presents 8.57% input THD and 2.05% at the load.

The sensitivity analysis also indicates that moderate values of N_2 provide a suitable compromise between control performance and computational effort. Therefore, selecting an intermediate N_2 value can be considered a practical design guideline for real-time implementation of the proposed ASMPC strategy in multimodular matrix converter systems.

4. Conclusions

The ASMPC allows efficient switching between current tracking and reactive power minimization without requiring the tuning of weighting factors typically needed in conventional MPC strategies. The simulation results show good reference tracking and low harmonic distortion, achieving an input current THD of 8.10% and a load THD of 1.00%, while maintaining stable performance under variations of the N_2 parameter.

The low dispersion observed in the evaluated metrics confirms that the system performance is not compromised by changes in N_2. This invariance simplifies the controller design and reinforces the robustness of the proposed strategy, positioning ASMPC as an efficient control solution for multimodular matrix converter systems.

Author Contributions: Conceptualization, R.R., M.R., S.T. and E.M.; methodology, S.T. and R.R.; software, R.R., S.T. and M.R.; validation, R.R., S.T. and C.R.; formal analysis, E.M., S.T. and R.R.; investigation, R.R. and C.R.; resources, E.M., S.T., M.R. and R.G.; writing—original draft preparation, R.R.; writing—review and editing, E.M., S.T., M.R., R.G., C.R. and S.N.; supervision, E.M., S.T., M.R. and R.G. All authors have read and agreed to the published version of the manuscript.

Funding: This research was supported by the National Council of Science and Technology (CONACYT), Paraguay

Data Availability Statement: All the data used are made available in the present work.

Acknowledgments: The authors sincerely thank the Doctorate Program in Electronic Engineering with an emphasis on Power Electronics at the National University of Asunción and the National Council for Science and Technology (CONACYT) of Paraguay, within the framework of projects POSG01-14, and PINV01-743. This work was supported by the Consejo Nacional de Ciencia y Tecnología (CONACYT) of Paraguay under Strategic Project ESTR01-3. We also acknowledge the A7C200 IRCF Project from the University of Nottingham and the Programa de Redução de Asimetrias na Pós-Graduação (PRAPG) – Edital nº 14/2023 – DRI – CAPES. ID Number: 046.821.818-15.

Conflicts of Interest: The authors declare no conflicts of interest.

References

1. Ali, M.; Iqbal, A.; Khalid, M. A review on recent advances in matrix converter technology: Topologies, control, applications, and future prospects. *Int. J. Energy Res.*, **2023**, 6619262. [CrossRef]
2. von Jouanne, A.; Agamloh, E.; Yokochi, A. A review of matrix converters in motor drive applications. *Energies* **2025**, *18*, 164. [CrossRef]
3. Priya Darshini, Y.S.; Ranga Reddy, G.P.; Bhavana, A.; Bhanusri, B.; Jahnavi, M.; Navitha, G. Matrix converter modeling in DFIG based wind system. In Proceedings of the 2024 10th International Conference on Advanced Computing and Communication Systems (ICACCS), Coimbatore, India, 14–16 March 2024; pp. 1328–1333. [CrossRef]
4. Wang, R.; Huang, M.; Lu, C.; Wang, W. A direct three-phase AC-AC matrix converter-based wireless power transfer system for electric vehicles. *Appl. Sci.* **2020**, *10*, 2217. [CrossRef]
5. Malekjamshidi, Z.; Jafari, M.; Zhu, J.; Rivera, M.; Soong, W. Model predictive control of the input current and output voltage of a matrix converter as a ground power unit for airplane servicing. *Sustainability* **2021**, *13*, 9715. [CrossRef]
6. Wang, J. High-Power Multimodular Matrix Converters and Modulation. Ph.D. Thesis, Ryerson University, Toronto, ON, Canada, 2012. [CrossRef]
7. Zhang, J.W.; Wang, Y.H.; Liu, G.C.; Tian, G.Z. A review of control strategies for flywheel energy storage system and a case study with matrix converter. *Energy Rep.* **2022**, *8*, 3948–3963. [CrossRef]
8. Toledo, S.; Caballero, D.; Maqueda, E.; Arrua, S.; Gomez-Redondo, M.; Gregor, R.; Rivera, M.; Wheeler, P. Fault-tolerant predictive control for six-phase wind generation systems using multi-modular matrix converter. In Proceedings of the IECON 2021—47th Annual Conference of the IEEE Industrial Electronics Society, Toronto, ON, Canada, 13–16 October 2021; pp. 1–6. [CrossRef]
9. Wheeler, P.W.; Rodriguez, J.; Clare, J.C.; Empringham, L.; Weinstein, A. Matrix converters: A technology review. *IEEE Trans. Ind. Electron.* **2002**, *49*, 276–288. [CrossRef]
10. Monteiro, J.; Pinto, S.; Delgado Martin, A.; Silva, J.F. A new real-time Lyapunov-based controller for power quality improvement in unified power flow controllers using direct matrix converters. *Energies* **2017**, *10*, 779. [CrossRef]

11. Tian, Y.; Zhang, Y.; Liu, C.; Xiao, X. Weighting factors design of model predictive control for three-level inverter-fed PMSM drives using multi-objective particle swarm optimization and artificial neural network. *IEEE Access* **2024**, *12*, 128641–128651. [CrossRef]
12. He, T.; Wu, M.; Lu, D.D.-C.; Wang, S.; Zhu, J. Fuzzy-based model predictive control for bidirectional charging of EV: An adaptive weighting factor algorithm. In Proceedings of the 2023 IEEE International Future Energy Electronics Conference (IFEEC), Sydney, Australia, 27–30 November 2023; pp. 284–287. [CrossRef]
13. Song, W.; Yang, Y.; Qin, W.; Wheeler, P. Switching state selection for model predictive control based on genetic algorithm solution in an indirect matrix converter. *IEEE Trans. Transp. Electrific.* **2022**, *8*, 4496–4508. [CrossRef]
14. Zhang, J.; Norambuena, M.; Li, L.; Dorrell, D.; Rodriguez, J. Sequential model predictive control of three-phase direct matrix converter. *Energies* **2019**, *12*, 214. [CrossRef]
15. Zhang, J.; Rivera, M.; Wheeler, P. Alternating sequential model predictive control of matrix converter. In Proceedings of the 2023 IEEE International Conference on Predictive Control of Electrical Drives and Power Electronics (PRECEDE), Wuhan, China, 16–19 June 2023; pp. 1–6. [CrossRef]
16. Khosravi, M.; Amirbande, M.; Khaburi, D.A.; Rivera, M.; Riveros, J.; Rodriguez, J.; Vahedi, A.; Wheeler, P. Review of model predictive control strategies for matrix converters. *IET Power Electron.* **2019**, *12*, 3021–3032. [CrossRef]
17. Romero, R.; Toledo, S.; Romero, C.; Caballero, D.; Quinonez, E.; Nunez, S.; Maqueda, E.; Renault, A.; Gregor, R.; Rivera, M. Fault-tolerant predictive current control with input reactive power minimization in six-phase generation system driven by a multi-modular matrix converter. In Proceedings of the 2022 IEEE International Conference on Automation/XXV Congress of the Chilean Association of Automatic Control (ICA-ACCA), Curicó, Chile, 24–28 October 2022; pp. 1–6. [CrossRef]
18. Rivas-Martínez, G.I.; Rodas, J.; Doval-Gandoy, J. Statistical tools to evaluate the performance of current control strategies of power converters and drives. *IEEE Trans. Instrum. Meas.* **2021**, *70*, 1006111. [CrossRef]
19. Rivas-Martínez, G.I.; Rodas, J.; Herrera, E.; Doval-Gandoy, J. A novel approach to performance evaluation of current controllers in power converters and electric drives using non-parametric analysis. *IEEE Lat. Am. Trans.* **2025**, *23*, 68–77. [CrossRef]
20. Posada Hernández, G.J. *Elementos Básicos de Estadística Descriptiva para el Análisis de Datos*; Fondo Editorial, Fundación Universitaria Luis Amigó: Medellín, Colombia, 2016; ISBN 978-958-8943-05-3.
21. de la Puente Viedma, C. *Estadística Descriptiva e Inferencial y una Introducción al Método Científico*; UNED–Universidad Nacional de Educación a Distancia: Madrid, Spain, 2020; ISBN 978-84-362-7641-2.